

# Extraction of keratin from wool and its use as biopolymer in film formation and in electrospinning for composite material processing

Sahil Goyal<sup>1</sup>, Marius Dotter<sup>2</sup>, Elise Diestelhorst<sup>2</sup>, Jan Lukas Storck<sup>2</sup> ,  
Andrea Ehrmann<sup>2</sup>  and Boris Mahltig<sup>1</sup> 

## Abstract

Keratin is one of the most important protein materials and can act as a sustainable biopolymer for manifold applications. This paper reports on a sustainable extraction method for keratin from wool fiber materials. The use of this extracted keratin for polymer film preparation and preparation of nano-composite materials by electrospinning is investigated. The preparation of keratin films is done in combination with the both biopolymers alginate and pectin. Keratin nanofibers are prepared in combination with the polymer polyacrylonitrile PAN. A view on antibacterial properties of the prepared films is given. As further analytic methods, Fourier-transform infrared (FT-IR) spectroscopy, thermogravimetry, and scanning electron microscopy (SEM) are used. Finally, the preparation of new keratin containing materials is described, which may be used in future for biomedical applications.

## Keywords

Keratin, wool, electrospinning, SEM, FT-IR spectroscopy, antimicrobial, antibacterial

Date received: 14 December 2021; accepted: 11 March 2022

## Introduction

Due to reasons of sustainability and environmental safety, recently there is a growing interest in the production and use of bio-based materials.<sup>1,2</sup> Such materials from renewable resources can be mainly categorized into three different groups according to their chemical basic structure. These categories are polysaccharides, lipids, and proteins.<sup>3</sup>

From these three groups, protein-based biomaterials have emerged as promising candidates for many biomedical applications, because they can act as an extracellular matrix that can promote cell-cell and cell-matrix interaction.<sup>4–6</sup>

Moreover, for many biomedical applications where biocompatibility is important protein-based materials are attractive, due to their biocompatible properties. In the production of biopolymers, numerous proteins have been

studied in recent years, important examples are collagen, albumin, gelatin, fibroin, and keratin. Due to their intrinsic biocompatibility, biodegradability, mechanical toughness, and natural abundance, keratin-based materials are promising in the biomedical field.<sup>7,8</sup>

Keratin is the main structural protein of hair, horn, and feathers.<sup>9–11</sup> Keratin is often also classified as cysteine

<sup>1</sup>Faculty of Textile and Clothing Technology, Niederrhein University of Applied Sciences, Mönchengladbach, Germany

<sup>2</sup>Faculty of Engineering and Mathematics, Bielefeld University of Applied Sciences, Bielefeld, Germany

### Corresponding author:

Boris Mahltig, Hochschule Niederrhein – Campus Monchengladbach, Webschulstr. 31, Mönchengladbach 41065, Germany.

Email: boris.mahltig@hs-niederrhein.de



sulfur-crosslinked fibrous protein.<sup>10</sup> Especially mentioned should be wool as keratin source. Wool from lower quality is often gained after meat production and can be used as keratin source for other applications.<sup>12</sup> Probably, keratin is the most abundant non-food protein.<sup>13</sup> For this, waste containing keratin can be seen as essential renewable resource that can be used by biopolymer pooling and processing. At present, keratin-based biomass is often disposed, because burning for energy production is inefficient and lead to burning gases containing also  $\text{NO}_x$  and  $\text{SO}_2$ . Keratin contains a high sulfur content (2.5–6 wt-%) which is related to the formation of  $\text{SO}_2$  in the burning gas.<sup>10</sup>

Earlier, the preparation of protein films from wool extracted keratin were used to investigate the structural and biological properties of self-assembled keratins. The properties of products made from extracted wool keratins were investigated in the year 1996 by Yamauchi et al.<sup>14</sup>

Other studies show that keratin is useful in a rapid casting technique for preparing protein films.<sup>15–17</sup> The feasibility of integrating such bioactive molecules as alkaline phosphatase into keratin films for controlled-release applications is also revealed in this earlier research.<sup>15</sup> Nevertheless, often the films had low strength and versatility. Studies on keratin films then moved to concentrate on improving the physical strength and versatility of films while retaining their biological activity.<sup>8,18</sup> Several approaches, including the addition of natural and synthetic polymers to keratin blended systems and new preparation methods for pure keratin films, have been considered for regulating physical and biological properties.<sup>8,17,19</sup> To gain a fully bio-based material, only natural polymers have to be used for this film preparation.

Pectin and alginate both polyuronates, are suitable examples in this area. The combination of keratin with alginate is reported for the production of blended films.<sup>20,21</sup> These two biopolymers support chain-chain interaction and form hydrogels when divalent cations are added to them. Alginates are structural polysaccharides which are gained by extraction of brown algae. Alginates consist of guluronic (G) and mannuronic (M) acid as molecular building blocks. The ratio of M- and G-blocks depends on the type of natural source.<sup>10,22</sup>

Pectin, one of the biggest constituents of citrus by-products, is a significant structural component of plant cell walls alongside cellulose and hemicelluloses.<sup>10</sup> The basic structure of pectin is the linear polymer of 1,4-linked d-galacturonic acid, in which some monomer units are esterified with a methyl group.<sup>10</sup> Like alginates, low methoxyl pectins, form gels with divalent cations.<sup>23,24</sup> Pectin finds application as a gelling or thickening agent.<sup>25</sup>

Beside using keratin for film preparation, this material can be also used as a component to prepare nanofibers by an electrospinning process. In this field, fiber materials from keratin and polyethylene oxide (PEO) are reported earlier by combination of aqueous keratin solutions with

PEO powder.<sup>9,26</sup> These researchers identified the electrospinning parameters in the first of two experiments to produce defect-free fibrous materials. In order to compare the chemical, physical, and rheological properties of the mixing solutions with the morphological, structural, thermal, and mechanical properties of the electro spun mats, keratin and PEO were mixed in various proportions. Compared to both pure PEO and keratin, the keratin/PEO solutions are shown to have increased viscosities, and the blends exhibited a non-Newtonian flow behavior with strong shear-thinning properties that were dependent on the PEO concentration. However, the practical uses of the nanofibrous keratin/PEO mats have ultimately been restricted by their water instability and weak mechanical properties.<sup>27</sup>

With this background, it is the objective of this study to use an environmentally friendly method for keratin production by extraction from wool and to evaluate possible applications for this keratin material. For this keratin extraction non-toxic solvents are used, following the approach of Wang et al.<sup>28</sup> who use water-based solutions of the natural amino acid cysteine and urea for keratin extraction. In recent years, other groups reported the use of cysteine containing recipes for keratin extraction.<sup>29,30</sup> In a second step, blended films from the extracted keratin together with the biopolymers alginate and keratin are developed. The antibacterial properties of the prepared film materials are investigated. Finally, the use of the extracted keratin in electrospinning processes together with water-stable poly(acrylonitrile) (PAN) is evaluated.

## Experimental section

### Extraction of keratin

The used extraction procedure is performed according to the report of Wang et al.<sup>28</sup> from year 2016. The wool used for keratin extraction is cleaned by using a Soxhlet extraction with petroleum ether, followed by a rinsing with distilled water. For keratin extraction, the cleaned wool fibers are cut into units with a length of 2 mm. Afterward, 5 g of the cut fibers are placed in 100 mL of an aqueous solution containing 8 mol/L urea and 0.165 mol/L L-cysteine. This solution is set to pH 10.5 by adding 5 M NaOH dropwise. Afterward, the solution is shaken at 75°C for 5 h. The chemicals are supplied by following companies; urea from Sigma Aldrich, L-cysteine from Merck, and sodium hydroxide from Carl Roth GmbH (Karlsruhe, Germany).

The obtained solution is filtered and cleaned by dialysis against distilled water for 3 days at room temperature. For dialysis a tube with an average pore size of 2.5–3 nm is used (Nadir-Dialyses Schlauch, Carl Roth GmbH, Karlsruhe, Germany), as similarly described in a previous publication.<sup>31</sup> The distilled water is adjusted four times a day. Photographs of the dialysis tube after different duration of dialysis are shown in Figure 1. The change in coloration of

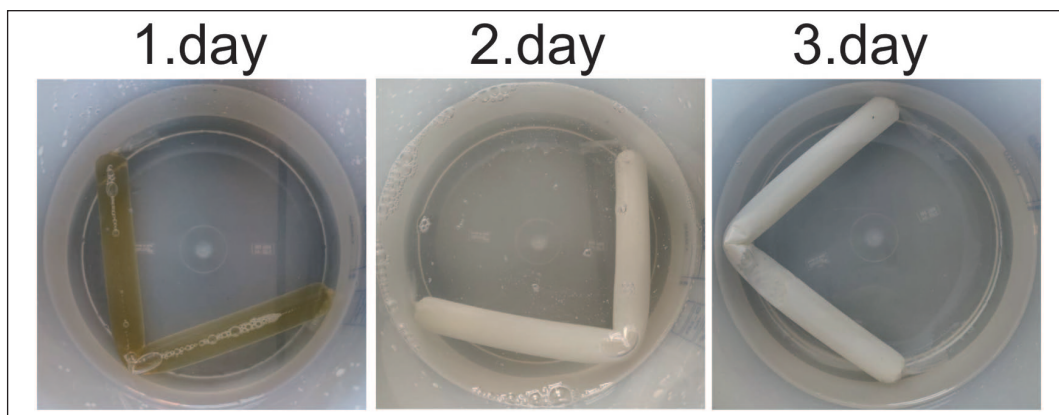


**Figure 1.** Photographs of dialysis tubes after different durations of dialysis.

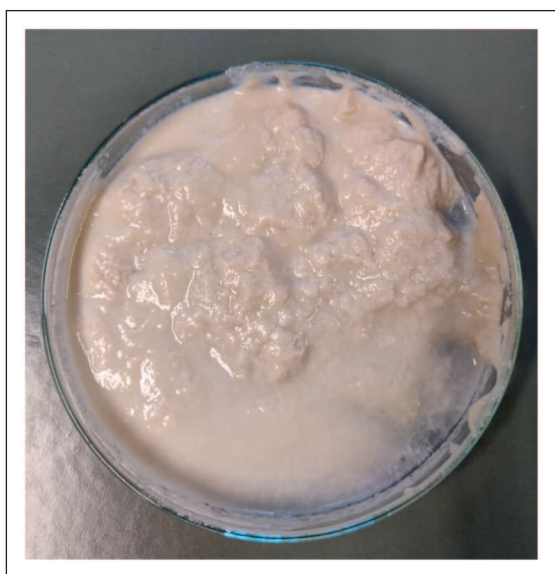


**Figure 2.** Photograph showing the pure keratin gained after filtration.

the liquid is obvious. After 3 days of dialysis, the pH of the solution is adjusted to 4.0–4.5 by addition of diluted acetic acid. Under these acidic conditions, the solid keratin precipitates from this solution. The precipitated keratin is filtered off, by using a standard filtration paper (see Figure 2). Subsequently, centrifugation and drying is performed to gain keratin powder. The drying is performed at room temperature.

### Preparation of films

The gels for casting films are prepared by dissolving the polymers (alginate, pectin, and keratin) in distilled water containing glycerin with a constant stirring at 1000 rpm for 2–3 h at 40°C. The concentrations of the solutions are given in Table 1. These homogenized gels are kept for at least 1 h at room temperature until all air bubbles are

**Table 1.** Compositions used for film formation with increasing amount of keratin content.

Trial no.	Trial 1	Trial 2	Trial 3	Trial 4
Sodium Alginate (g)	2.5	2.5	2.5	2.5
Pectin (g)	2.5	2.5	2.5	2.5
Glycerin (g)	2.5	2.5	2.5	2.5
Keratin (g)	–	1	2	3
Formic acid (mL)	–	5	5	5
Deionized water (mL)	92.5	86.5	85.5	84.5

eliminated. The blank films are dried cast by pouring the gel (20 g) into a plastic Petri dish (d=90 mm). Afterward, drying is performed at 45°C for 48 h. The keratin-loaded polymeric films are prepared by addition of 5 mL of formic acid solution. The compositions used for film formation are summarized in Table 1. The keratin content in the films is set in the range up to 3%. These keratin-loaded films are as well dried at 45°C. The film formation process is shown exemplarily in Figure 3.

### Electrospinning

Electrospinning is used to produce nanofibers of keratin in combination with polyacrylonitrile (PAN). For this, solutions of 15% PAN (copolymer with 6% methyl methacrylate, X-PAN, Dralon, Dormagen, Germany) in the solvent DMSO ( $\geq 99.9\%$ , S3 chemicals, Bad Oeynhausen, Germany) are prepared by stirring for 2 h at room temperature. This PAN is often used as a precursor for carbon nanofibers, with typical amounts of 15–16 wt% solid content in the solution to gain straight fibers at the below mentioned spinning conditions.<sup>32–34</sup> To these solutions, keratin is added in increasing concentrations of 1.9 wt%, 3.3 wt%, 4.7 wt%, and 6.1 wt%. Higher keratin concentrations could not be electrospun. Electrospinning is performed by a wire-based electrospinning machine Nanospider Lab (Elmarco, Liberec, Czech Republic), using the following

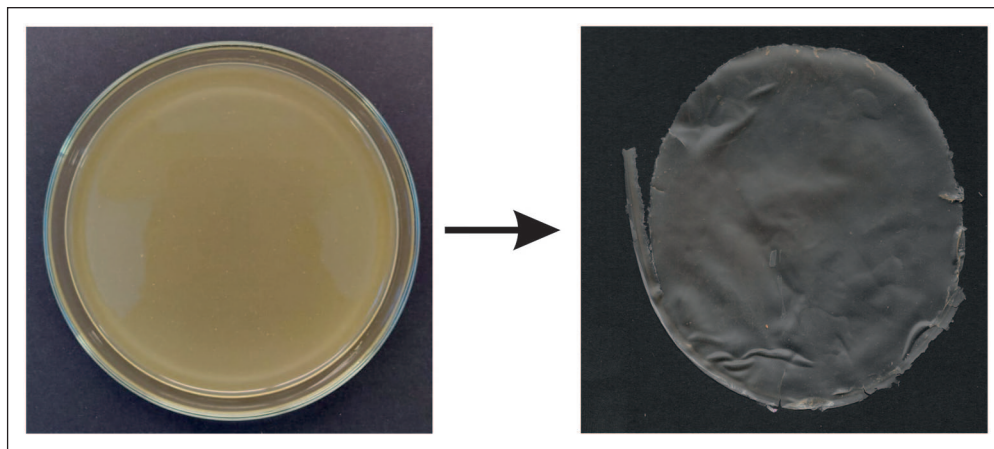


**Figure 3.** Photograph for documentation of film formation process – left: solution in the petri dish; right: the finally gained film.

spinning parameters: voltage 70 kV, electrode–substrate distance 230 mm, nozzle diameter 0.8 mm, carriage speed 100 mm/s, substrate speed 0 mm/min, relative humidity and temperature in the spinning chamber 32% and 22°C–23°C, respectively, and spinning duration of 30 min.

### Analytic methods

FTIR spectroscopy is performed using the device Excalibur 3100 supplied by Varian Inc. (USA), which is equipped with an attenuated total reflection (ATR) unit, and an Excalibur 3100 (Varian Inc., Palo Alto, CA, USA) in ATR mode. The spectra cover a frequency range from 4000 to 700  $\text{cm}^{-1}$ . Each spectrum is averaged over 32 scans and corrected for atmospheric noise.

Thermogravimetric (TGA) and calorimetric (DSC) measurements are done using a TGA/DSC 2500 Regulus device supplied by Netzsch (Germany). These measurements are performed under argon atmosphere. In addition, a Hi-Res TGA 2950 Thermo-gravimetric Analyzer from TA Instruments (New Castle, DE, USA) and a DSC 3 device by Mettler-Toledo (Gießen, Germany) with a nitrogen atmosphere are used, respectively.

Scanning electron microscopy SEM is performed using a microscope Tabletop TM 4000Plus supplied by Hitachi (Japan). Fiber diameters are evaluated from these images using ImageJ (Software version 1.53e, 2021, National Institutes of Health, Bethesda, MD, USA).

The antibacterial activities are tested according to the standard of AATCC 147-2004 (parallel streak method) against the two bacteria species *Staphylococcus aureus* and *Klebsiella pneumoniae*. These antibacterial tests are performed with the prepared polymer films. For this test, the plates are prepared by pouring 15 mL of sterilized agar onto sterile Petri plates. The agar plates are allowed to solidify for 5 min and the bacterial culture is inoculated

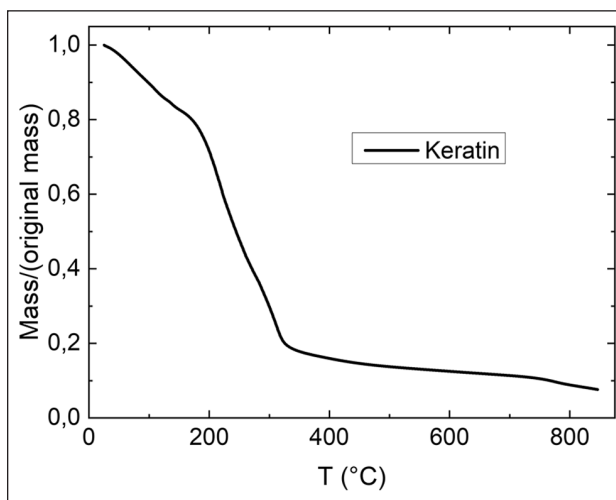


**Figure 4.** Thermogravimetric analysis (TGA) of the produced keratin. The decrease of sample mass is shown as a function of increasing temperature.

as single lines. The polymer films are cut into small pieces and are laid over the inoculated bacterial species with a diameter of 2.5 cm. These plates are incubated at 37°C for 24 h.

### Results and discussion

The prepared keratin – shown as substance in Figure 2 – is used as a component for the preparation of two different materials, bio-based polymer films and composite nanofiber mats. Both materials are presented in the following sub-sections. The thermal properties of the prepared keratin are described by thermogravimetric measurements (TGA), with results shown in Figures 4 and 5. During heating till 170°C the weight loss of keratin is constantly on a lower level with less than 0.2%/K. This decrease is

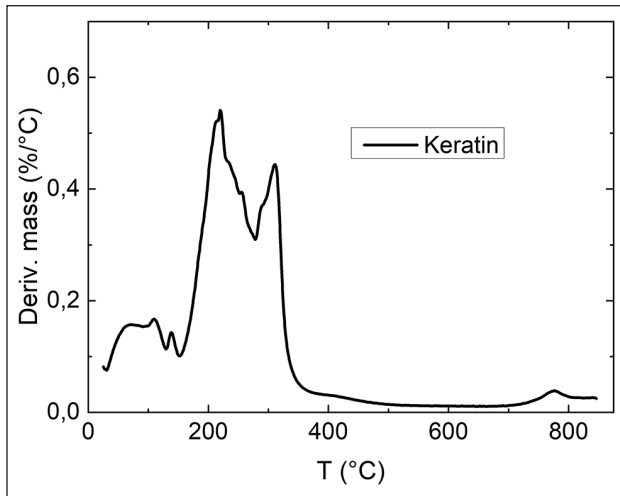


**Figure 5.** Thermogravimetric analysis (TGA) of the produced keratin. The change of sample mass at a distinct temperature is shown.

probably related to the release of bonded water, so this could be named as a kind of drying process.<sup>35</sup> Heating above 200°C of the keratin sample leads to a strongly increased mass loss until a temperature of 350°C is reached, because in this temperature range, the thermal degradation of keratin occurs.<sup>35</sup>

### Film formation with keratin and antibacterial properties

The film preparation is done with keratin under addition of the biopolymer's alginate and pectin. These three components as well as the polymer film built up by them are investigated by FT-IR spectroscopy (Figures 6 and 7). Due to the protein structure of keratin, its infrared spectrum is mainly determined by peaks related to the vibrations of the N-monosubstituted amide groups.<sup>36</sup> The peaks at 1615 and 1593  $\text{cm}^{-1}$  can be correlated to the amide signals Amide I and Amide II, which are related to C=O stretching vibration and a combination of stretching vibration of C-N with a deformation vibration of C-N-H.<sup>37,38</sup> The signal at 782  $\text{cm}^{-1}$  can be correlated to the Amide V signal, which is related to a deformation vibration of N-H (Figure 6).<sup>37</sup> Of course, keratin as a protein is not only built up by amide groups; the side groups also exhibit several different functional groups leading to manifold other IR signals.<sup>39</sup>

The IR spectra of pectin and alginate as polysaccharides are mainly determined by the stretching vibrations of O-H (around 3260  $\text{cm}^{-1}$ ), C-H (around 2900  $\text{cm}^{-1}$ ), and C-O bonds (around 1015  $\text{cm}^{-1}$ ) (Figure 6). Nevertheless, both components are produced from natural products and depending on the natural source used for production, IR-spectra with typical differences can be recorded.<sup>40</sup>

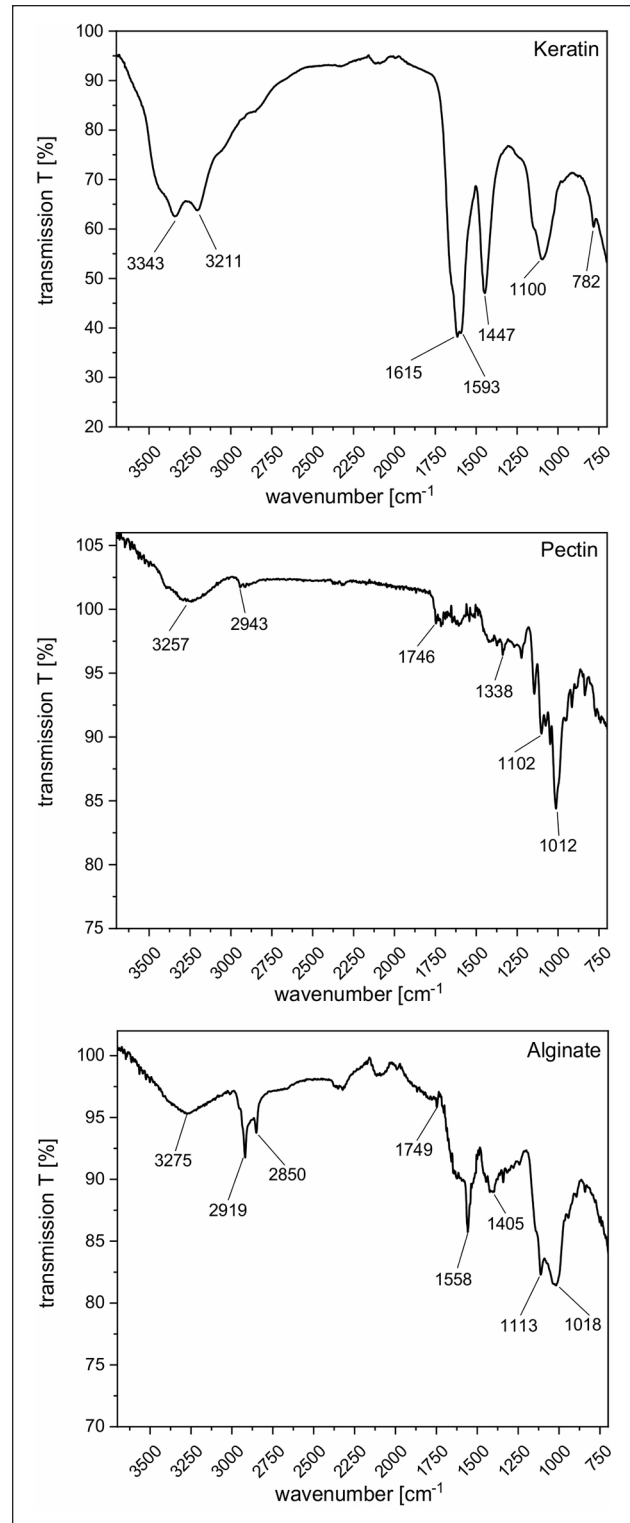


**Figure 6.** FT-IR spectra of the prepared keratin and both substances used for film preparation – pectin and alginate.

In case of pectin the IR-signal at 1746  $\text{cm}^{-1}$  can be correlated to C=O stretching vibration of an ester group as a result of the methyl esterification of pectin.<sup>41</sup>

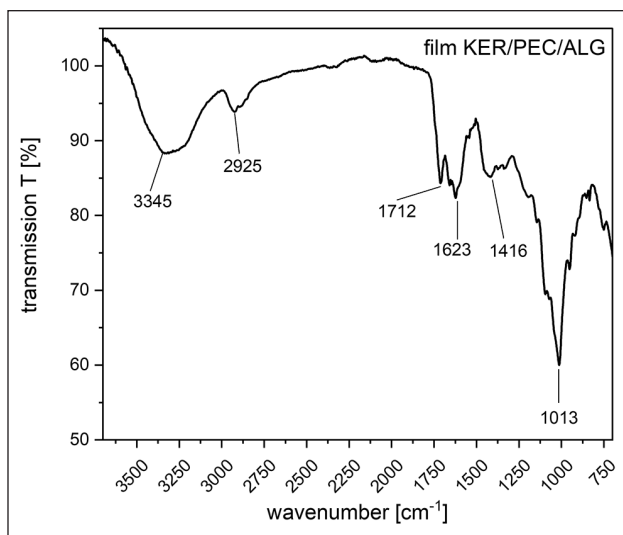


**Figure 7.** FT-IR spectrum of the prepared film containing the three components – keratin (KER), pectin (PEC), and alginate (ALG).

The IR spectrum of the prepared film from keratin, pectin, and alginate is presented in Figure 7. This spectrum exhibits two clear signals at 1712 and 1623  $\text{cm}^{-1}$ , which can be correlated to the two components pectin and keratin used for film preparation. The signal at 1712  $\text{cm}^{-1}$  is probably related to C=O stretching vibration of the ester group in pectin and the signal at 1623  $\text{cm}^{-1}$  is related to the Amide I signal of keratin.

Further, the prepared films are microscopically investigated by SEM (Figure 8). Here, the surface topography of a film containing only alginate and pectin is compared with the surface of a film containing all three components – including keratin. The macroscopic appearance of both films is nearly the same. However, on a microscopic scale they show completely different topography (Figure 8). The polymer film from alginate and pectin exhibit a smoother topography, which could also be described as a cloudy appearance. In contrast, the film containing additional keratin shows a topography which is determined by the presence of small ellipsoidal units which are randomly distributed on the surface. Probably, these units are related to crystallized keratin areas.

Using the parallel streak method, the antibacterial properties of the prepared films against the bacteria *S. aureus* and *K. pneumoniae* are evaluated (Figures 9 and 10). There is no clear inhibition zone for growth of both the bacteria in case of the film prepared from alginate and pectin (Figure 9). However, when the bacteria are exposed to the keratin containing film, a slightly visible inhibition zone is present for both *S. aureus* and *K. pneumoniae* (Figure 10). Of course, this determined effect is not that

strong compared to keratin or other materials which are especially doped with antimicrobial agents, as for example, nanosilver.<sup>42–44</sup>

### Electrospinning of keratin composite fibers

The electrospun PAN/keratin nanofiber mats were firstly investigated by SEM to evaluate the nanofiber morphology. Figure 11 depicts images taken with different magnifications on the nanofibrous composites.

In all cases, nanofibers are produced, as the images with higher magnification (right panels) reveal. Nevertheless, there are also beads visible along the fibers, especially for the lower keratin concentrations. These beads are typical for electrospun nanofiber mats with relatively low viscosity and high surface tension.<sup>45–47</sup> Here, they are reduced or completely avoided for larger keratin contents.

The images with lower magnification (left panels), however, show additional large stains on the nanofiber mats. These stains are partly also visible in the background of the higher magnified images, for example, for 1.9% keratin. While the smaller beads along the nanofibers, as visible in the higher magnifications for 1.9% keratin and 3.3% keratin, respectively, can be attributed to the interaction between electrical charges along the jet and surface energy during electrospinning,<sup>48</sup> the larger stains stem from an additional electrospinning process which does not occur for pure PAN nanofibers and can thus be attributed to the keratin content of the spinning solutions.<sup>46</sup> These stains are not fixed to a specific nanofiber, but cover the nanofiber mat at the surface and, as visible for 1.9% keratin (large magnification), also below.

The influence of the keratin content on the fiber diameters is depicted in Figure 12. For larger keratin contents, the diameters show a broader distribution with a larger average diameter. Average diameters are  $(210 \pm 100)$  nm (1.9% keratin),  $(220 \pm 90)$  nm (3.3% keratin),  $(320 \pm 190)$  nm (4.7% keratin), and  $(450 \pm 210)$  nm (6.1% keratin), respectively. Depending on the spinning solutions and parameters, sometimes slightly narrower distributions are reported, while broader distributions including strong deviations from normal distributions can also be found in the literature.<sup>49,50</sup>

DSC measurements of these samples are presented in Figure 13. For pure keratin, the broad peak around 100°C can be attributed to evaporation of bound water, while the second broad peak around 190°C–270°C indicates keratin polypeptide chain denaturation.<sup>51</sup> In the PAN/keratin nanofiber mats, the first endothermic peak can be correlated with evaporation of the solvent DMSO.<sup>52</sup> Further PAN-related peaks are not expected below 270°C.<sup>53</sup> Thus the small residual endothermic peaks around 190°C and 225°C can be attributed to the keratin fraction of the nanofiber mats.

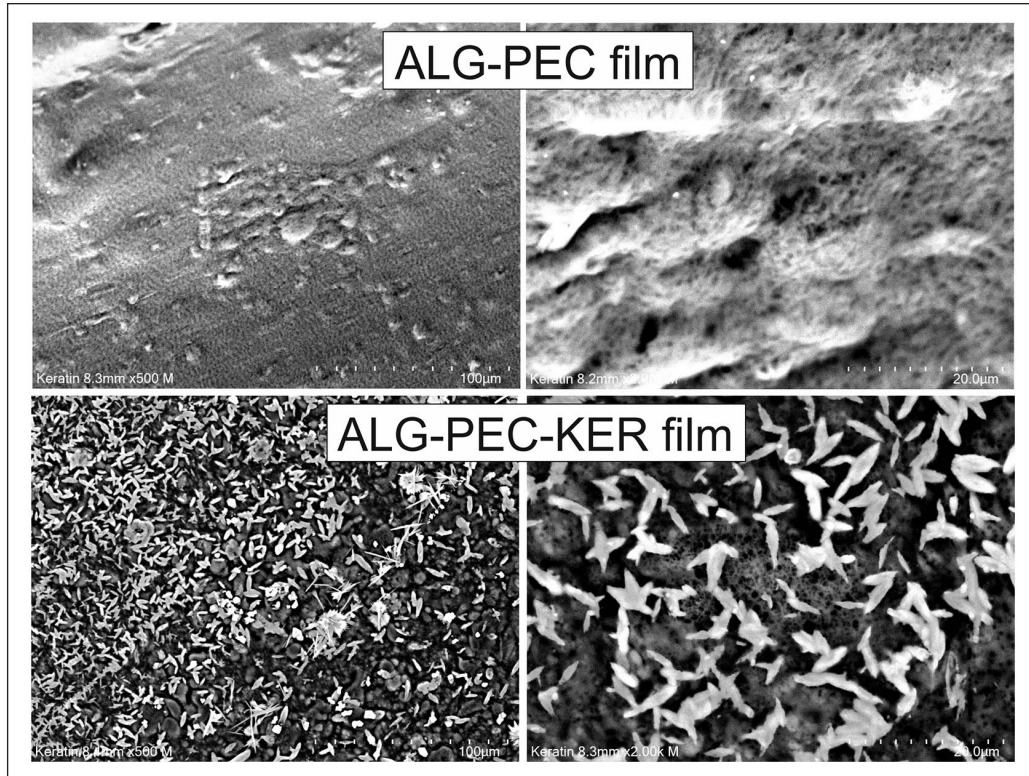


**Figure 8.** SEM-images of the produced films, from alginate and pectin (top row) and from alginate, pectin, and keratin (bottom row). For the samples, images recorded in two different magnifications are shown (left images with low magnification and right images with high magnification).

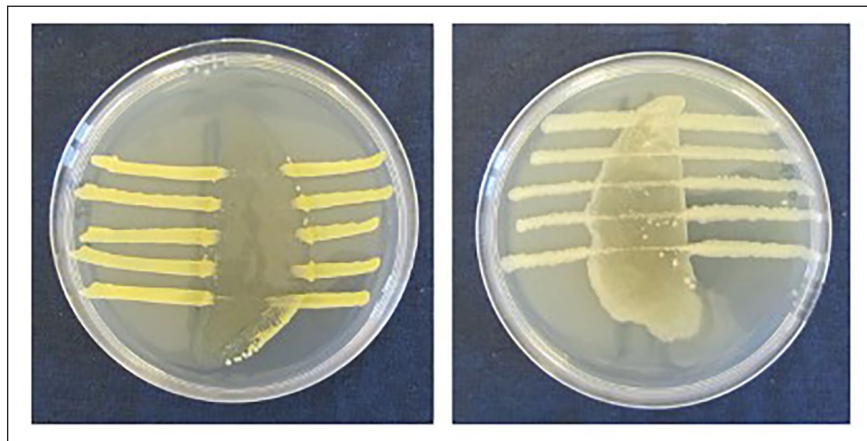


**Figure 9.** Agar plates with prepared films from alginate and pectin after the antibacterial test – left: test with *S. aureus*; right: test with *K. pneumoniae*.

Finally, Figure 14 depicts FTIR spectra of the nanofiber mats with different amounts of keratin. The graphs show on the one hand the typical PAN peaks, such as  $\text{-C}\equiv\text{N}$  stretching at  $2245\text{ cm}^{-1}$  and  $\text{-CH}_2$  bending at  $1452\text{ cm}^{-1}$ , slightly decreasing for larger keratin contents.<sup>36–38</sup> On the

other hand, the typical keratin peaks like  $\text{C=O}$  stretching at  $1720\text{ cm}^{-1}$  and  $\text{CO}_2$  asymmetric stretching  $1560\text{ cm}^{-1}$  are visible, showing that both materials form composite nanofiber mats, as expected. Quantification of FTIR results is generally problematic in case of thin nanofiber

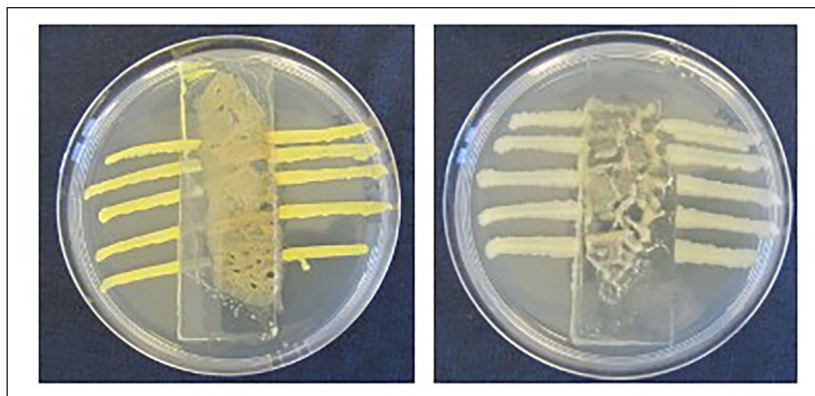


**Figure 10.** Agar plates with prepared films from keratin alginate and pectin after the antibacterial test – left: test with *S. aureus*; right: test with *K. pneumoniae*.

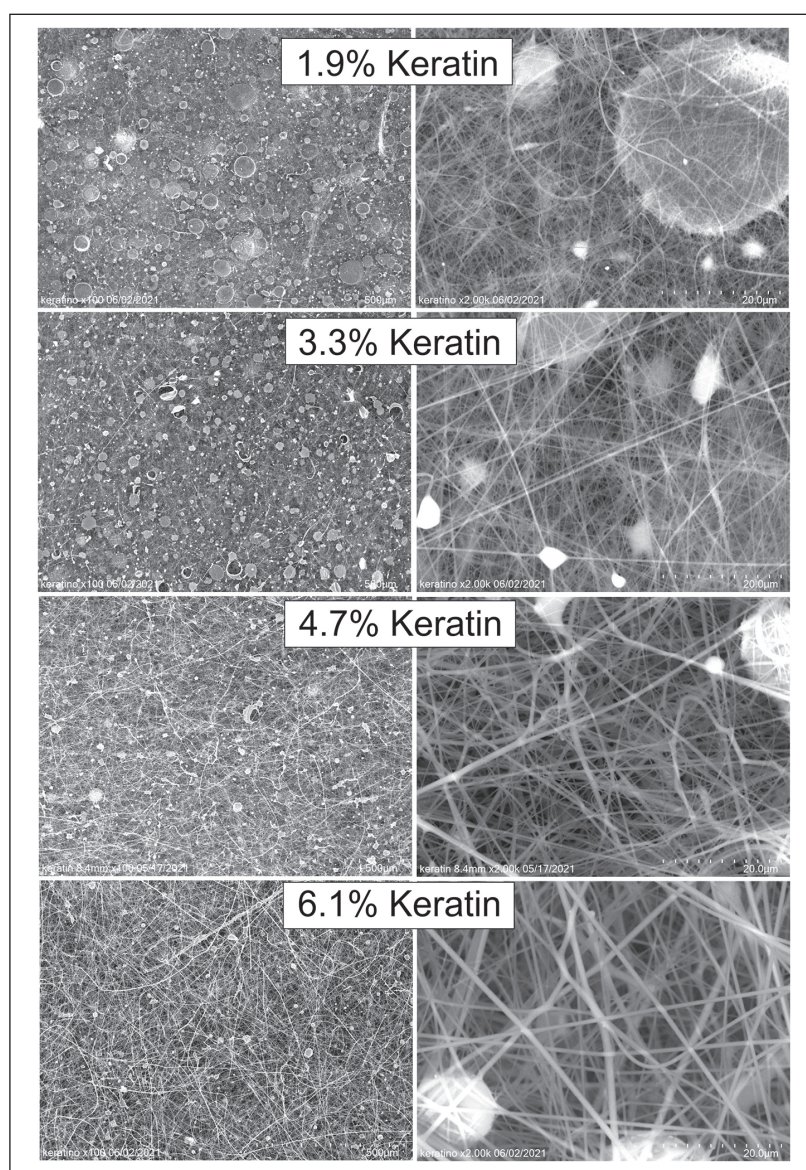


**Figure 11.** SEM-images of electrospun keratin/PAN fibers. The content of Keratin in the spinning solution is indicated in the images. For each sample images recorded in two different magnifications are shown (left images with low magnification and right images with high magnification).



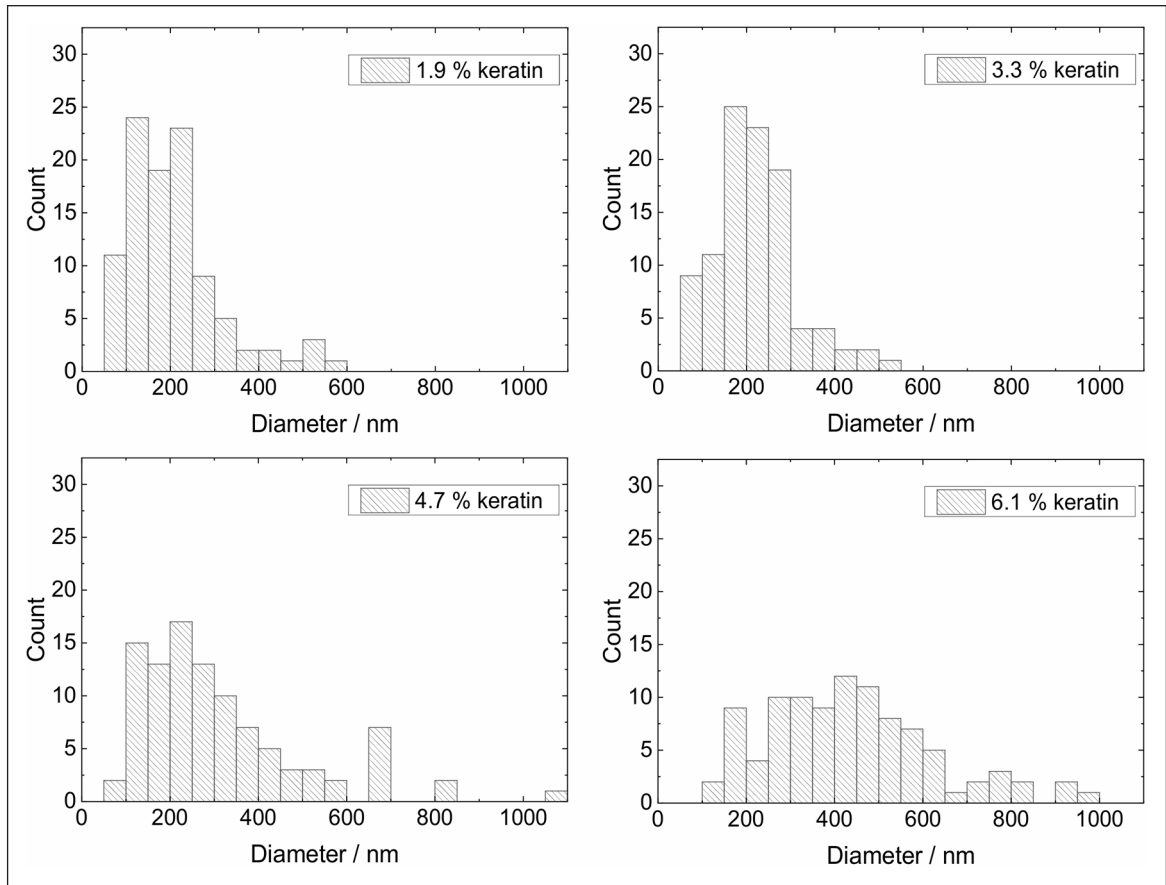


**Figure 12.** Distribution of fiber diameters of electrospun keratin/PAN fibers determined by evaluation of the SEM-images. The content of keratin in the spinning solution is indicated in each graph.

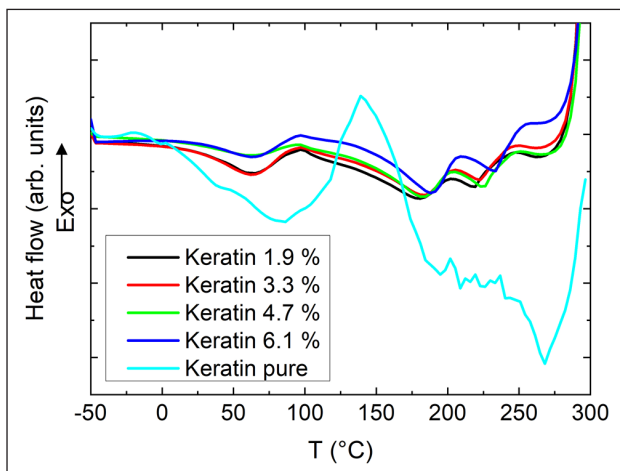


**Figure 13.** DSC measurements of the electrospun keratin/PAN fibers in comparison to a pure keratin sample.

mats where often artifacts are visible. However, since an increase in the wt% of keratin can only result in a decrease in the wt% of PAN in the final, solid nanofiber mat without solvent residues, this quantification is not believed to be necessary here.

## Conclusions

Keratin material is extracted from wool by using a sustainable extraction method. This keratin can be used as raw material for polymer film preparation and preparation of nano-composite materials by electrospinning. A slight antibacterial effect is determined for the prepared polymer films containing keratin. In the future such fully bio-based polymer films and the composite nanofiber could be promising components for the preparation of materials with application in the biomedical field.

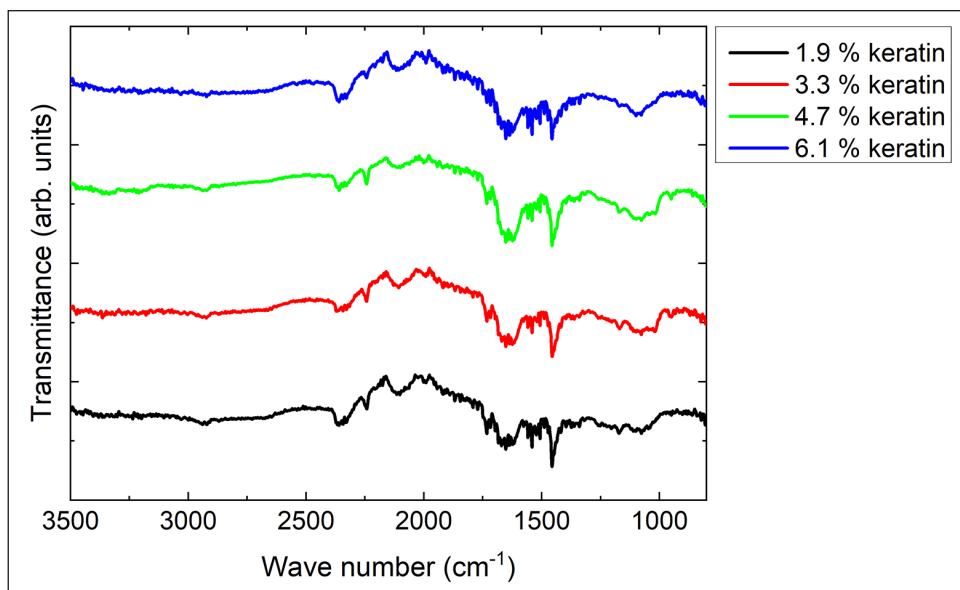


**Figure 14.** Infrared spectra of the electrospun keratin/PAN fibers.

### Acknowledgements

For help in the lab and useful discussions the authors owe many thanks to Mister T. Heistermann, Dipl.-Ing. G. Lieutenant-Bister, Dr. E. Rohleder and Dipl.-Biol. B. Hildenberg (Hochschule Niederrhein, Mönchengladbach, Germany).

### Declaration of Conflicting Interests

The author(s) declared no potential conflicts of interest with respect to the research, authorship, and/or publication of this article.

### Funding

The author(s) received no financial support for the research, authorship, and/or publication of this article.

### ORCID iDs

Jan Lukas Storck  <https://orcid.org/0000-0002-6841-8791>

Andrea Ehrmann  <https://orcid.org/0000-0003-0695-3905>

Boris Mahltig  <https://orcid.org/0000-0002-2240-5581>

### References

- Babu RP, O'Connor K and Seeram R. Current progress on bio-based polymers and their future trends. *Prog Biomater* 2013; 2(1): 8.
- RameshKumar S, Shaiju P, O'Connor KE, et al. Bio-based and biodegradable polymers - state-of-the-art, challenges and emerging trends. *Curr Opin Green Sustain Chem* 2020; 21:75–81.
- Jastorff B, Störmann R and Wölcke U. *Struktur-Wirkungs-Denken in der Chemie: Eine Chance für mehr Nachhaltigkeit*. Oldenburg: Isensee, 2003.
- Gagner JE, Kim W and Chaikof EL. Designing protein-based biomaterials for medical applications. *Acta Biomater* 2014; 10:1542–1557.
- Silva NHCS, Vilela C, Marrucho IM, et al. Protein-based materials: from sources to innovative sustainable materials for biomedical applications. *J Mater Chem B* 2014; 2(24): 3715–3740.
- Agnieray H, Glasson JL, Chen Q, et al. Recent developments in sustainably sourced protein-based biomaterials. *Biochem Soc Trans* 2021; 49(2): 953–964.
- Rouse JG and Van Dyke ME. A review of keratin-based biomaterials for biomedical applications. *Materials* 2010; 3(2): 999–1014.
- Feroz S, Muhammad N, Ranayake J, et al. Keratin - based materials for biomedical applications. *Bioact Mater* 2020; 5(3): 496–509.
- Fan J, Lei T, Yu M, et al. Keratin/PEO/hydroxyapatite nanofiber membrane with improved mechanical property for potential burn dressing application. *Fibers Polym* 2020; 21(2): 366–375.
- Ebert G. *Biopolymere*. Stuttgart: Teubner, 1993.
- Fan J and Yu WD. High yield preparation of keratin powder from wool fiber. *Fibers Polym* 2012; 13(8): 1044–1049.
- Brown EM, Pandya K, Taylor MM, et al. Comparison of methods for extraction of keratin from waste wool. *Agric Sci* 2016; 7(10): 670–679.
- Zoccola M, Aluigi A and Tonin C. Characterisation of keratin biomass from butchery and wool industry wastes. *J Mol Struct* 2009; 938(1–3): 35–40.
- Yamauchi K, Yamauchi A, Kusunoki T, et al. Preparation of stable aqueous solution of keratins, and physicochemical and biodegradational properties of films. *J Biomed Mater Res* 1996; 31(4): 439–444.

15. Fujii T, Ogiwara D and Arimoto M. Convenient procedures for human hair protein films and properties of alkaline phosphatase incorporated in the film. *Biol Pharm Bull* 2004; 27(1): 89–93.
16. Thonpho A and Srihanam P. Preparation and characterization of keratin blended films using biopolymers for drug controlled release application. *Orient J Chem* 2016; 32(4): 1739–1748.
17. Katoh K, Shibayama M, Tanabe T, et al. Preparation and physicochemical properties of compression-molded keratin films. *Biomaterials* 2004; 25(12): 2265–2272.
18. Rajabi M, Ali A, McConnell M, et al. Keratinous materials: structures and functions in biomedical applications. *Mater Sci Eng C* 2020; 110:110612.
19. Rajabinejad H, Zoccola M, Patrucco A, et al. Physicochemical properties of keratin extracted from wool by various methods. *Text Res J* 2018; 88(21): 2415–2424.
20. He M, Zhang B, Dou Y, et al. Blend modification of feather keratin-based films using sodium alginate. *J Appl Polym Sci* 2017; 134(15): 44680.
21. Cazón P, Velazquez G, Ramírez JA, et al. Polysaccharide-based films and coatings for food packaging: a review. *Food Hydrocolloids* 2017; 68:136–148.
22. Trueb F. *Pflanzliche Naturstoffe*. Stuttgart: Gebr. Borntraeger Verlagsbuchhandlung, 2015.
23. Wellner N, Kačuráková M, Malovíková A, et al. FT-IR study of pectate and pectinate gels formed by divalent cations. *Carbohydr Res* 1998; 308(1–2): 123–131.
24. Matia-Merino L, Lau K and Dickinson E. Effects of low-methoxyl amidated pectin and ionic calcium on rheology and microstructure of acid-induced sodium caseinate gels. *Food Hydrocolloids* 2004; 18(2): 271–281.
25. Willats WGT, Knox JP and Mikkelsen JD. Pectin: new insights into an old polymer are starting to gel. *Trends Food Sci Technol* 2006; 17(3): 97–104.
26. Aluigi A, Varesano A, Montarsolo A, et al. Electrospinning of keratin/poly(ethylene oxide)blend nanofibers. *J Appl Polym Sci* 2007; 104(2): 863–870.
27. Aluigi A, Vineis C, Varesano A, et al. Structure and properties of keratin/PEO blend nanofibres. *Eur Polym J* 2008; 44(8): 2465–2475.
28. Wang K, Li R, Ma JH, et al. Extracting keratin from wool by using L-cysteine. *Green Chem* 2016; 18(2): 476–481.
29. Zhang N, Wang Q, Yuan J, et al. Highly efficient and eco-friendly wool degradation by L-cysteine-assisted esperase. *J Clean Prod* 2018; 192:433–442.
30. Pourjavaheri F, Ostovar Pour S, Jones OAH, et al. Extraction of keratin from waste chicken feathers using sodium sulfide and L-cysteine. *Process Biochem* 2019; 82:205–214.
31. Mahltig B, Greiler LC and Haase H. Microwave assisted conversion of an amino acid into a fluorescent solution. *Acta Chim Slov* 2018; 65:865–874.
32. Sabantina L, Klöcker M, Wortmann M, et al. Stabilization of polyacrylonitrile nanofiber mats obtained by needleless electrospinning using dimethyl sulfoxide as solvent. *J Ind Text* 2020; 50(2): 224–239.
33. Sabantina L, Rodríguez-Cano MÁ, Klöcker M, et al. Fixing PAN nanofiber mats during stabilization for carbonization and creating novel metal/carbon composites. *Polymers* 2018; 10:735.
34. Haider A, Haider S and Kang I-K. A comprehensive review summarizing the effect of electrospinning parameters and potential applications of nanofibers in biomedical and biotechnology. *Arab J Chem* 2018; 11(8): 1165–1188.
35. Sharma S, Gupta A, Kumar A, et al. An efficient conversion of waste feather keratin into ecofriendly bioplastic film. *Clean Technol Environ Policy* 2018; 20(10): 2157–2167.
36. Hesse M, Meier H and Zeeh B. *Spectroscopic methods in organic chemistry*. Stuttgart: Georg Thieme Verlag, 2008.
37. Günzler H and Gremlich H-U. *IR spectroscopy*. Weinheim: Wiley-VCH, 2002.
38. Mahltig B. High-performance fibres – a review of properties and IR-Spectra. *Tekstilec* 2021; 64(2): 96–118.
39. Vasconcelos A, Freddi G and Cavaco-Paulo A. Biodegradable materials based on silk fibroin and keratin. *Biomacromolecules* 2008; 9(4): 1299–1305.
40. Leal D, Matsuhiro B, Rossi M, et al. FT-IR spectra of alginic acid block fractions in three species of brown seaweeds. *Carbohydr Res* 2008; 343(2): 308–316.
41. Fellah A, Anjukandi P, Waterland MR, et al. Determining the degree of methylesterification of pectin by ATR/FT-IR: methodology optimisation and comparison with theoretical calculations. *Carbohydr Polym* 2009; 78(4): 847–853.
42. Gaidau C, Petica A, Ciobanu C, et al. Investigations on antimicrobial activity of collagen and keratin based materials doped with silver nanoparticles. *Rom Biotechnol Lett* 2009; 14(5): 4665–4672.
43. Haase H, Fahmi A and Mahltig B. Impact of silver nanoparticles and silver ions on innate immune cells. *J Biomed Nanotechnol* 2014; 10(6): 1146–1156.
44. Barani H and Mahltig B. Using microwave irradiation to catalyze the in-situ manufacturing of silver nanoparticles on cotton fabric for antibacterial and UV-protective application. *Cellulose* 2020; 27:9105–9121.
45. Ehrmann A. Non-toxic crosslinking of electrospun gelatin nanofibers for tissue engineering and biomedicine—a review. *Polymers* 2021; 13(12): 1973.
46. Grothe T, Storck JL, Dotter M, et al. Impact of solid content in the electrospinning solution on the physical and chemical properties of polyacrylonitrile (PAN) nanofibrous mats. *Tekstilec* 2020; 63(3): 225–232.
47. Haghi AK and Akbari M. Trends in electrospinning of natural nanofibers. *Phys Stat Sol A* 2007; 204(6): 1830–1834.
48. Reneker DH and Yarin AL. Electrospinning jets and polymer nanofibers. *Polymer* 2008; 49(10): 2387–2425.
49. Malašauskienė J and Milašius R. Mathematical analysis of the diameter distribution of electrospun nanofibres. *Fiber Text East Eur* 2010; 18:45–48.
50. Malašauskiene J, Milašius R and Kuchanauskaitė E. Possibilities for the estimation of electrospun nanofibre diameter distribution by Normal (Gaussian) distribution. *Fibres Text East Eur* 2016; 24:23–28.
51. Monteiro VF, Maciel AP and Longo E. Thermal analysis of caucasian human hair. *J Therm Anal Calorim* 2005; 79(2): 289–293.
52. Bonora S, Markarian SA, Trincherio A, et al. DSC study on the effect of dimethylsulfoxide (DMSO) and diethylsulfoxide (DESO) on phospholipid liposomes. *Thermochim Acta* 2005; 433(1–2): 19–26.
53. Zhang G, Chen L, Qiu L, et al. Preparation and characterization of poly (Acrylonitrile-co-1-Acryloylpyrrolidine-2-Carboxylic acid) with high molecular weight. *J Macromol Sci Part B* 2013; 52(9): 1298–1308.